

Functional divergence in the proteins encoded by *ARO80* from *S. uvarum*, *S. kudriavzevii* and *S. cerevisiae* explain differences in the aroma production during wine fermentation

Sebastián M. Tapia,¹  Roberto Pérez-Torrado,¹ 
Ana Cristina Adam,¹  Laura G. Macías,^{1,2} 
Eladio Barrio^{1,2}  and Amparo Querol¹ 

¹Departamento de Biotecnología de los Alimentos, Grupo de Biología de Sistemas en Levaduras de Interés Biotecnológico, Instituto de Agroquímica y Tecnología de Los Alimentos (IATA)-CSIC, 46980, Valencia, Spain.

²Departament de Genètica, Universitat de València, Valencia, Spain.

Summary

Phenylethanol (PE) and phenylethyl acetate (PEA) are commonly desired compounds in wine because of their rose-like aroma. The yeast *S. cerevisiae* produces the PE either through de novo biosynthesis by shikimate pathway followed by the Ehrlich pathway or the direct phenylalanine catabolism via Ehrlich pathway, and then converted into PEA. Previous work demonstrated that, compared to *S. cerevisiae*, other *Saccharomyces* species, such as *S. kudriavzevii* and *S. uvarum*, produce higher concentrations of PE and PEA from the precursor phenylalanine, which indicates differential activities of the biosynthetic-involved enzymes. A previous in-silico analysis suggested that the transcriptional activator Aro80p is one of the best candidates to explain these differences. An improved functional analysis identified significant radical amino acid changes in the *S. uvarum* and *S. kudriavzevii* Aro80p that could impact the expression of the catabolic genes *ARO9* and *ARO10*, and hence, the production of PE from

phenylalanine. Indeed, wine *S. cerevisiae* strains carrying the *S. uvarum* and *S. kudriavzevii* *ARO80* alleles increased the production of both compounds in the presence of phenylalanine by increasing the expression of *ARO9* and *ARO10*. This study provides novel insights of the unidentified Aro80p regulatory region and the potential usage of alternatives *ARO80* alleles to enhance the PE and PEA concentration in wine.

Introduction

Saccharomyces cerevisiae is frequently used as a starter culture in winemaking since it is adapted to a variety of stresses that occur during fermentation (Pretorius, 2000; Querol *et al.*, 2018). Nowadays, to solve the problems of the production of higher alcohol wines, as a consequence of the adverse effects of climate change and to adjust to the current consumer preference trends, other species of the genus, such as *Saccharomyces uvarum* and *Saccharomyces kudriavzevii*, as well as their interspecific hybrids with *S. cerevisiae*, can be used as suitable alternative starter yeasts (Querol *et al.*, 2018). These yeasts have been associated with wine fermentation and display desired enological traits of interest to solve the global warming effect on the wine production, such as lower ethanol yields, higher glycerol synthesis, good fermentation performance at low temperatures and the generation of interesting aroma profiles (González *et al.*, 2007; Gamero *et al.*, 2013; Pérez-Torrado *et al.*, 2015). The most important aroma compounds produced by yeast during fermentation are higher alcohols and acetate esters which highly impact wine's flavour and aroma (Ugliano and Henschke, 2009). Higher (or fusel) alcohols are synthesized by yeast from the catabolism of aromatic, branched and sulphur-containing amino acids through Ehrlich pathway (Hazelwood *et al.*, 2008; Ugliano and Henschke, 2009; Cordente *et al.*, 2012). These alcohols can subsequently be transformed into their acetate esters by the action of acetyltransferases encoded by the genes *ATF1* and *ATF2* which, together with the esterase *Iah1p*, modulate their final concentration (Ugliano and Henschke, 2009;

Received 23 January, 2022; revised 19 April, 2022; accepted 24 April, 2022.

For correspondence. E-mail aquerol@iata.csic.es; Tel. +34 963900022; Fax +34 963636301.

Microbial Biotechnology (2022) 15(8), 2281–2291

doi:10.1111/1751-7915.14071

Funding Information

This project has received funding from the European Union's Horizon 2020 research and innovation programme under the Marie Skłodowska-Curie grant agreement number 764364, Aromagenesis, and from the Spanish government and EU ERDF-FEDER projects RTI2018-093744-B-C31 and RTI2018-093744-B-C32 to AQ and EB respectively.

© 2022 The Authors. *Microbial Biotechnology* published by Society for Applied Microbiology and John Wiley & Sons Ltd.

This is an open access article under the terms of the Creative Commons Attribution-NonCommercial-NoDerivs License, which permits use and distribution in any medium, provided the original work is properly cited, the use is non-commercial and no modifications or adaptations are made.

Cordente *et al.*, 2012). Among these compounds, 2-phenylethanol (PE) and 2-phenylethyl acetate (PEA) are commonly desired in the wine because of their pleasant rose-like aroma that positively contributes to the wine's aromatic profile (Ugliano and Henschke, 2009). PE biosynthesis via Ehrlich pathway (Kim *et al.*, 2014; Qian *et al.*, 2019) begins with the transamination of the aromatic amino acid phenylalanine into phenylpyruvate by the aromatic aminotransferase II Aro9p. Part of the phenylpyruvate also proceeds from the sugar catabolism (Rollero *et al.*, 2019), in which, the glycolytic flux enters to the shikimate pathway to generate chorismite (Gientka and Duszkiwicz-Reinhard, 2009), and then, transformed into phenylpyruvate that finally enters to the Ehrlich pathway. Then, the phenylpyruvate is decarboxylated to phenylacetaldehyde by the broad-substrate-specificity 2-keto acid decarboxylase Aro10p. Finally, phenylacetaldehyde is reduced into PE through the alcohol dehydrogenases Adh1p to Adh7p together with the formaldehyde dehydrogenase Sfa1p (Cordente *et al.*, 2012). PE is then either excreted to the medium or converted into PEA by acetyltransferases Atf1p and Atf2p. (Stribny *et al.*, 2015) reported that *S. kudriavzevii* and *S. uvarum* species produce higher concentrations of PE and PEA, respectively, from the aromatic amino acid phenylalanine than *S. cerevisiae*. Their results suggest differential activities of the enzymes involved in the aromatic compound biosynthetic pathways. To determine the molecular foundations that explain these differences, an in-silico analysis based on Grantham's score (Grantham, 1974) determined that Aro10p, Atf1p and Atf2p were good candidates because of their high scores (Stribny, 2016). This method quantifies how similar or dissimilar are two amino acids residues based on their physicochemical properties such as composition, polarity and molecular volume to predict their evolutionary distance. High values implies that both amino acids are evolutionary unlikely to be substituted with one another. Such replacements in a protein could potentially generate functional changes in their activity.

Previous studies demonstrated that *S. kudriavzevii* Aro10p and both *S. kudriavzevii*/*S. uvarum* Atf1p and Atf2p versions showed differential substrate preferences and activities compared to those *S. cerevisiae* counterparts (Stribny *et al.*, 2016a,2016b). Both *S. kudriavzevii* and *S. uvarum* Atf2p increased twofold activity against the PE compared to the *S. cerevisiae* Atf2p. In addition, the K_m of *S. kudriavzevii* and *S. uvarum* Atf1p are twofold and threefold higher than *S. cerevisiae* Atf1p using isoamyl alcohol as substrate respectively. Besides, The V_{max} value of both Atf1p non-*S. cerevisiae* species was two times lower than *S. cerevisiae* Atf1p. Moreover, these alleles changed the final aromatic compound composition in synthetic wine fermentations when they were expressed into an *S. cerevisiae* background (Stribny *et*

al., 2016a,2016b). Another protein that showed a high Grantham's score in both *S. uvarum* and *S. kudriavzevii* species was Aro80p (Stribny, 2016), which belongs to the zinc binuclear proteins family (Iraqi *et al.*, 1999; MacPherson *et al.*, 2006). Aro80p is constitutively bound to the cis UAS_{ARO} elements of both *ARO9* and *ARO10* genes (Lee and Hahn, 2013) and specifically induces their expression in the presence of aromatic amino acids (Iraqi *et al.*, 1999; Godard *et al.*, 2007).

Since Aro80p is directly related to the Ehrlich pathway, this study aimed to test the effect of *ARO80* *S. kudriavzevii*/*S. uvarum* alleles on the production of PE and PEA from phenylalanine compared to the *S. cerevisiae* allele. To attain this, we improved the functional divergence analysis based on the method developed by Macías *et al.* (2019), who refined the functional divergence method developed by Toft *et al.* (2009) by quantifying divergences according to Grantham's scores. This method allowed us to identify candidate amino acid changes in Aro80p that might explain the observed differences in the synthesis of PE and PEA. To demonstrate these observations, we generated *S. cerevisiae* strains carrying the *ARO80* *S. kudriavzevii*/*S. uvarum* alleles and we cultured them in the presence of precursor phenylalanine to decipher their impact on the expression of the genes *ARO9* and *ARO10* regulated by Aro80p.

Experimental procedures

Aro80p protein functional divergence analysis

ARO80 gene sequences from representative *Saccharomyces* isolates (Table 1) were used for the functional divergence analysis. The method, described elsewhere (Macías *et al.*, 2019), was used to identify amino acids in the predicted Aro80p sequences from *S. uvarum* (Aro80p-Su) and *S. kudriavzevii* (Aro80p-Sk) that have diverged significantly from the *Torulaspora delbrueckii*

Table 1. Strains used for the bioinformatics analysis and sources of the genomic sequences.

Strain	Specie	References
T73	<i>Saccharomyces cerevisiae</i>	Morard <i>et al.</i> (2019)
S288C	<i>Saccharomyces cerevisiae</i>	Goffeau <i>et al.</i> (1996)
Y9	<i>Saccharomyces cerevisiae</i>	Liti <i>et al.</i> (2009)
YPS128	<i>Saccharomyces cerevisiae</i>	Liti <i>et al.</i> (2009)
BMV58	<i>Saccharomyces uvarum</i>	Macías <i>et al.</i> (2021)
NPCC1290	<i>Saccharomyces uvarum</i>	Macías <i>et al.</i> (unpublished)
CECT12600	<i>Saccharomyces uvarum</i>	Macías <i>et al.</i> (2021)
CBS7001	<i>Saccharomyces uvarum</i>	Scannell <i>et al.</i> (2011)
CR85	<i>Saccharomyces kudriavzevii</i>	Macías <i>et al.</i> (2019)
ZP591	<i>Saccharomyces kudriavzevii</i>	Scannell <i>et al.</i> (2011)
CA111	<i>Saccharomyces kudriavzevii</i>	Macías <i>et al.</i> (2019)
IFO1802	<i>Saccharomyces kudriavzevii</i>	Scannell <i>et al.</i> (2011)
CBS1164	<i>Torulaspora delbrueckii</i>	Gordon <i>et al.</i> (2011)

output orthologue in these two species with respect to the homologous site in the *S. cerevisiae* sequences (Aro80p-Sc). Once all divergent amino acid sites were obtained, results were filtered by Grantham's scores (Grantham, 1974), to quantify the biochemical divergence between *S. uvarum*-*S. kudriavzevii* and *S. cerevisiae* amino acids. Those showing scores equal to or higher than 120 were considered as radical changes (Stribny, *et al.*, 2016; Macías *et al.*, 2019).

Yeast strains and growth conditions

The parental and engineered strains used in this study are listed in Table 2. The transformant *aro80* mutant and *ARO80* recombinant strains were grown at 30°C on selective YPD solid media (1% yeast extract, 2% peptone, 2% glucose, 2% agar) containing, respectively, 200 µg ml⁻¹ G418 and 100 µg ml⁻¹ nourseothricin. For aroma compound determination and the gene expression experiments, the cell was grown in YNB liquid media (0.17% yeast nitrogen base without amino acid and ammonium, 2% glucose) containing the desired amino acid.

Strains constructions

The deletion of the *ARO80* open reading frame (ORF) in the haploid strain AQ2775, that derives from the wine strain T73 (Querol *et al.*, 1992), was carried out through PCR-mediated gene disruption using *KanMX* cassette as a selection marker (Baudin *et al.*, 1993), which was PCR amplified from the pUG6 plasmid (Güldener *et al.*, 1996) using NZYtaq II DNA Polymerase (NZYTech, Lisbon, Portugal) following the provided instructions. The strains were transformed through the lithium acetate method (Gietz and Schiestl, 2007) and deletions were confirmed by PCR using the diagnostic primers (Table 3). The *aro80* mutant strain was used as the parental strain to generate the recombinant *ARO80* strains (Fig. 1, Table 2) through allele swapping by CRISPR-Cas9-mediated gene disruption (Stovicek *et al.*, 2017). The protospacer sequence against the *KanMX* cassette was designed according to

Doench *et al.* (2014) using the T73 genome sequence as reference. Then, the entire plasmid pRCC-N was amplified with primers carrying the protospacer sequence at their 5' ends by PCR (Generoso *et al.*, 2016) which was carried out with Phusion™ High-Fidelity Polymerase (Thermo Fisher Scientific, Vilnius, Lithuania) following the provided instructions. Before the addition to the transformation mix, 30 µl of the PCR product were treated with 10 U of DpnI (Thermo Fisher Scientific, Vilnius, Lithuania) for 3 h to guarantee the degradation of the pRCC-N plasmid template. The *KanMX* cassette at *ARO80* locus was swapped with the *ARO80* ORF alleles from the *S. uvarum* strain AQ2901, *S. kudriavzevii* strain AQ4013 and *S. cerevisiae* strain AQ2775, which were amplified by PCR using Phusion™ High-Fidelity Polymerase. The ORF allele swapping was confirmed by PCR analysis of total DNA extracted from nourseothricin-resistant transformant strains whose resistance against G418 antibiotic was lost and whose ability to grow in the presence of tryptophan as the sole nitrogen source was recovered (Iraqi *et al.*, 1999). The reinserted *ARO80* alleles sequences were checked through Sanger sequencing from Eurofins Genomics Mix2Seq service.

Quantification of 2-phenylethanol and 2-phenylethyl acetate production

To test PE and PEA production, the cells were incubated overnight in YNB liquid media containing 5 g l⁻¹ ammonium sulphate as nitrogen source and then inoculated in 80 ml of YNB liquid media containing either 12.5 g l⁻¹ phenylalanine or 5 g l⁻¹ ammonium sulphate as the sole nitrogen source (Stribny *et al.*, 2015) starting with 1 × 10⁶ cells ml⁻¹. Medium samples were collected after 48 h of cell growth when all glucose is depleted. To quantify the PE and PEA production in each sample, 5 ml of sample was mixed with 4.95 ml of 303 g l⁻¹ NaCl solution and 50 µl of 3-octanol as internal standard. Then passed it through a TRACE™ GC Ultra gas chromatograph (Thermo Fisher Scientific, Waltham, MA, USA) coupled with a flame ionization detector (FID), equipped with a 30 m × 0.25 mm × 0.25 µm HP-INNOWax capillary column coated with a layer of cross-linked polyethylene glycol (Agilent Technologies, Santa Clara, USA) at carrier gas helium flow rate of 1 ml min⁻¹. The oven temperature programme was: (i) five minutes at 50°C, (ii) temperature raised to 100°C at an increasing rate of 1.5°C min⁻¹. (iii) then up to 215°C at a rate of 3°C min⁻¹ and (iv) was kept for 2 min more. The FID detector temperature was 280°C and the aromatic compounds were identified by their retention time. Quantification was made by using calibration plots of the corresponding compounds.

Table 2. Strains used in this study.

Strain	Genotype	References
AQ2775	T73 <i>MATalpha</i>	This study
AQ2901	BMV58 <i>MATa</i>	This study
AQ4013	CR85 <i>MATalpha ho::MX4dsdA</i>	This study
ST44	<i>MATalpha, aro80::KanMX</i>	This study
ST44-Sc	<i>MATalpha, aro80::kanmx::ARO80(T73)</i>	This study
ST44-Su	<i>MATalpha, aro80::kanmx::ARO80(BMV58)</i>	This study
ST44-Sk	<i>MATalpha, aro80::kanmx::ARO80(CR85)</i>	This study

Table 3. Primers used in this study.

Primer	Sequence (5' to 3')
Primers for <i>ARO80</i> gene disruption	
aro80Δ-Fw(1)	<u>GCATAATAAGGTTACATTAAGCA</u> <u>CTGCTTTATCCTCTATG</u> <u>TAGAGATCTGTTAGCTTGCCT</u>
aro80Δ-Rv(1)	<u>GCGGTTGTCTTGGTTGATGACGT</u> <u>AATCTTTGATATCTAC</u> <u>GTTTTCGACACTGGATGGC</u>
Primers for <i>ARO80</i> allele swapping	
Protospacer incorporation in pRRC-N plasmid	
gRNA-KanMX-Fw(2)	<u>TGTTTTGCCGGGATCGCAG</u> <u>GAATTCCTTTGATATCTACTTT</u> <u>TAGAGCTAGAAATAGCAA</u> <u>GTTAAAATAAGG</u>
gRNA-KanMX-Rv(2)	<u>CTGCGATCCCCGGCAAAACA</u> <u>GATCATTATCTTTCACTGCGGAG</u>
Primer for <i>ARO80</i> alleles amplification as donor DNA	
ARO80-Sc-Fw	TCCACGCATAATAAGGTTACAT
ARO80-Sc-Rv	ATTTTTACGAATAGTGCGGTTG
ARO80-Sk-Fw(3)	<u>GCATAATAAGGTTACATTA</u> <u>AGCACTGCTTTATCC</u> <u>TCTATGTCTCCTAAGAGAAGATCC</u>
ARO80-Sk-Rv(3)	<u>GCGGTTGTCTTGGTTGATGACGTAA</u> <u>TTCTTTGATATCT</u> <u>ACTTATTACGTGTTACTGGCC</u>
ARO80-Su-Fw(3)	<u>GCATAATAAGGTTACATTAAGCACT</u> <u>GCTTTATCCTCT</u> <u>ATGTCTACTACCAAAGAGGATCC</u>
ARO80-Su-Rv(3)	<u>GCGGTTGTCTTGGTTGATGACGTAA</u> <u>TTCTTTGATATCTAC</u> <u>TTATTGGTGTGCAGCTGGC</u>
<i>continuation</i>	
Diagnostic primers	
ARO80-Sc-test-Fw	TTTTCGGAATCAACGAGAGTACA
ARO80-Sc-test-Rv	TTTTCAGTGGTTTTCGGTGTT
ARO80-Sk-test-Rv	ATCTGCTGTTCACTTTTGCT
ARO80-Su-test-Rv	CTGTTGGAACATAAGAGACATC
K2	GGGACAATTCAACGCGTCTG
Primers for relative quantification through qPCR	
ACT1-F	CTTACAACCTCCATCATGAAGTGTGA
ACT1-R	ATTTCCTTTTGCATTCTTTTCGGC
18S-F(4)	TTGCGATAACGAACGAGACC
18S-R(4)	CATCGCTTGAACCGATAG
ARO9-F	CCGTGTCATCCGTTTGGAGA
ARO9-R	TGGACTCAGCCATTGCCTTT
ARO10-F	GATTTGCGGTTTCTTTCGCA
ARO10-R	AATTCACAACCTAGGGCGG
Sequencing primers	
ARO80-Sc-test-Rv2	TTTTGATTCCTATGGCTCCTAG
ARO80-Sc-Seq_1	TAATGGAAGAAATCGGGAAAGT
ARO80-Sc-Seq_2	AAACGATGGAAATGAAAGCAAT
ARO80-Sc-Seq_3	CGAGGTATGTGGAATTAGCATA
ARO80-Sc-Seq_4	CCCCTGTTATTCTGTCTTTGTA
ARO80-Su-Seq_1	TAGCACAGAACAAAATGGGATA
ARO80-Su-Seq_2	TAAAGAAGGTGCGAAGGAAATA
ARO80-Su-Seq_3	AAACCTTTTCATCCCGAGATAA
ARO80-Su-Seq_4	TCTCGGAATGAAAGGTTTTAT
ARO80-Su-Seq_5	ATCAACAGATATTGCACCTCAGT
ARO80-Su-Seq_6	TCTTGGTTGATGACGTAATTCT
ARO80-Sk-Seq_1	CTGCTTTATCCTCTATGTCTCC
ARO80-Sk-Seq_2	ACCCATTTTCTCCGTTATACAA
ARO80-Sk-Seq_3	TTGTGCAAACGAGAATCTTAAC
ARO80-Sk-Seq_4	ACAGATATTGCACTCAGTTTTTA
ARO80-Sk-Seq_5	CCCCTGTTATTCTGTCTTTGTA

(1) Homologous sequences to *KanMX* from the pUG6 plasmid are underlined. (2) The underlined sequences stand for the protospacers. (3) Underlined sequences stand for the specific *ARO80* alleles sequences. (4) Primer sequences from (Pérez-Torrado *et al.*, 2016).

ARO9 and *ARO10* gene expression analysis by real-time qPCR

To monitor the expression pattern of both *ARO9* and *ARO10* genes in the recombinant *ARO80* strains, samples of cells growing in YNB 12.5 g l⁻¹ phenylalanine liquid media were taken at different times (10, 24, 30 and 48 h), frozen in liquid nitrogen and stored at -80°C until RNA extraction. The *aro80* mutant strain ST44 was used as a negative expression control. Total RNA was extracted using a Qiagen RNA extraction kit (Qiagen, Hilden, Germany) following the provided instructions. The RNA samples were treated with 10 U of DNase I (Roche, Mannheim, Germany) and 1 µg was used to generate cDNA using NZY First-Strand cDNA synthesis kit (NYZ-Tech, Lisbon, Portugal). The qPCR experiments were carried in the LightCycler® 480 Instrument (Roche, Mannheim, Germany). Expression of both *ARO9* and *ARO10* genes in every sample was normalised against the average expression of the housekeeping genes *ACT1* and ribosomal 18S rRNA. Afterwards, fold change expression in each sample value was determined as the binary logarithm (log-2) of expression in one sample respect to the average expression of all samples at time 10 h.

Statistical analyses

All One-way ANOVA and Tukey's multiple comparisons analyses were performed using GraphPad Prism version 8.01 for Windows 10, GraphPad Software, La Jolla California USA (www.graphpad.com).

Results

S. uvarum and *S. kudriavzevii* show a high number of radical amino acid changes in *Aro80p*

A previous study demonstrated high functional divergence in *Aro80p* amino acid sequences in the *S. uvarum* and *S. kudriavzevii* species compared to *S. cerevisiae* based on Grantham's scoring (Stribny, 2016). In this study, we have used a different approach taking advantage of a new method, recently described (Macías *et al.*, 2019), to identify both evolutionary and functional significant radical amino acid changes in the *Aro80p*. These results (Fig. 2, Table S1) highlight the change D₄₅A_{45/56} which is shared by both species and located at the C₆ zinc-finger of the DNA-binding domain region. Furthermore, the *Aro80p*-Sk exhibits four changes in the middle region where the change N₅₀₂Y₅₀₆ is at a similar position to the N₅₀₂C₅₁₇ showed by *Aro80p*-Su, although the function of that region remains unclear. Other changes in *Aro80p*-Su are widespread along the protein sequence. The changes R₆G₁₇, S₁₁₄L₁₂₅ and N₁₇₀C₁₈₁ are located at the N-terminal end of the zinc finger

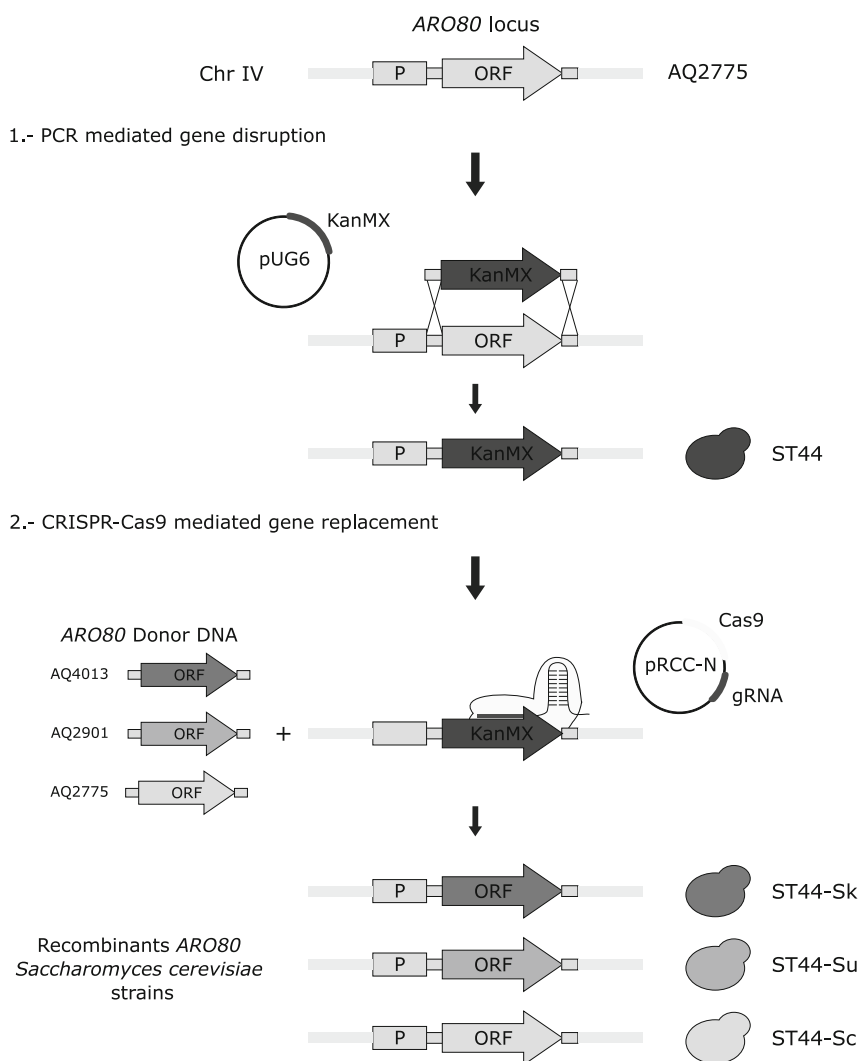


Fig. 1. Two-step *ARO80* allele swapping approach used for recombinant strain generation. (1) The *ARO80* open reading frame was deleted by PCR-mediated gene disruption using *KanMX* cassette. (2) The marker was replaced by CRISPR-Cas9 mediated gene disruption and the amplified *ARO80* alleles were used as donor DNA to ensure homologous recombination.

region, at the linker and the dimerization domain of the protein respectively. The change N₉₃₉I₉₅₄ is located between the C-terminal end and the acidic region, essential for recruiting the transcriptional machinery. Finally, the amino changes Y₅₃₂C₃₆₇ and G₆₉₀C₇₀₅ are in regions of unknown functions. Altogether, these changes could explain differences in the function of Aro80p-Sk and Aro80p-Su with respect to the *S. cerevisiae* protein.

Effect of ARO80 alleles on phenylethanol and phenylethyl acetate production

To determine the impact of the different *ARO80* alleles on the production of PE and PEA, we generated recombinant strains carrying the *S. uvarum* (ST44-Su), *S. kudriavzevii* (ST44-Sk) and *S. cerevisiae* (ST44-Sc)

ARO80 alleles. The parental *aro80* mutant strain (ST44) was used as a control. Strains were grown in a minimal medium containing either ammonium sulphate or the aromatic precursor phenylalanine and we quantified PE and PEA production after 48 h when all glucose was consumed (Fig. 3, Table S2). We observed that both recombinant strains ST44-Su and ST44-Sk increased the PE basal production by 11.2% and 13.4% compared to ST44-Sc strain in the presence of ammonium sulphate as the sole nitrogen source respectively. While the strain ST44 showed a 28.3% reduction of PE production. However, no PEA production was detected by any strain in this condition. Meanwhile, the strains ST44-Su and ST44-Sk increased the PE production by 12.7% and 13.1% and PEA production by 29% and 32.2%, respectively, compared to ST44-Sc in the presence of the

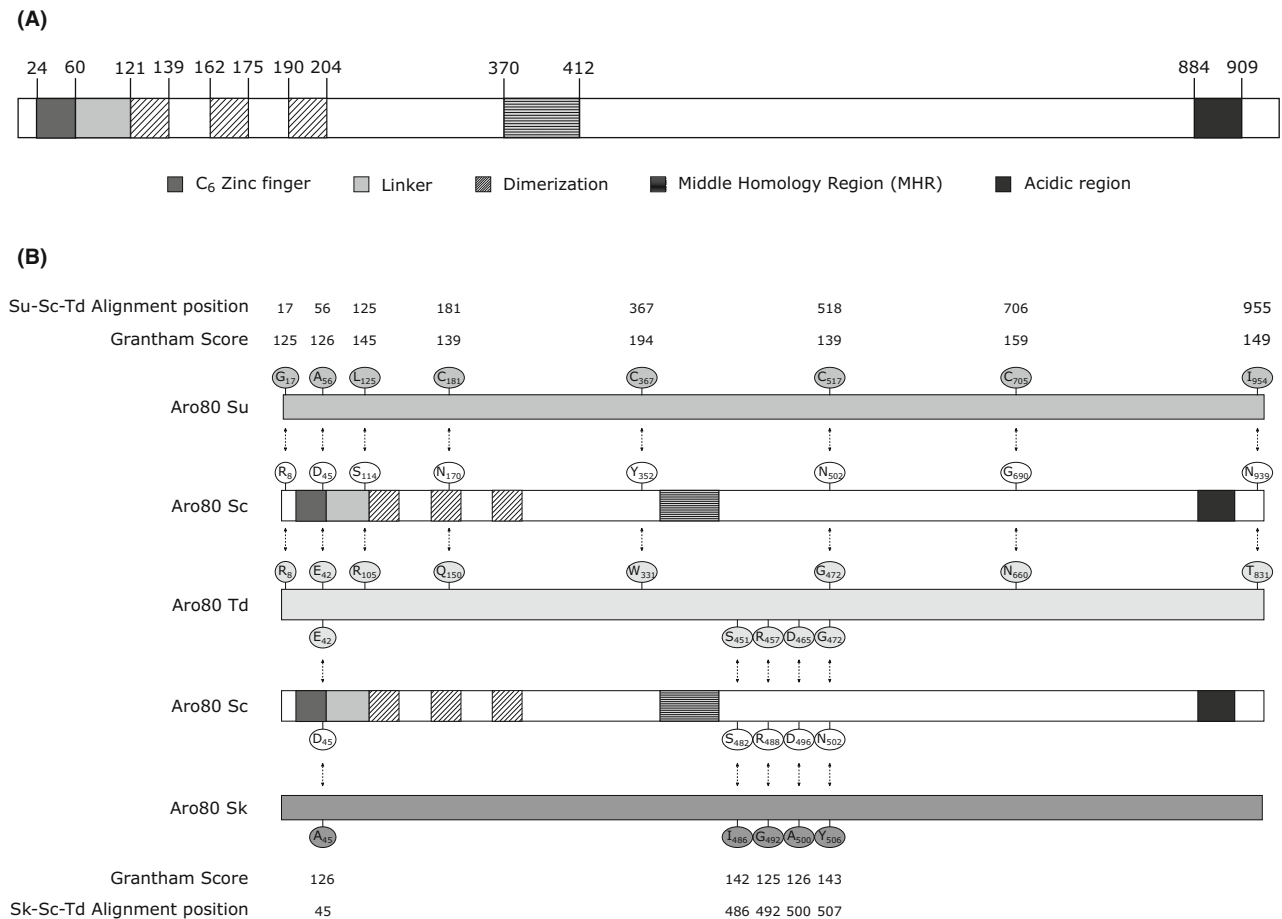


Fig. 2. Radical amino acids changes were observed in Aro80p comparing different *Saccharomyces* species.

A. Aro80p functional domains identified in *S. cerevisiae* by (Schjerling and Holmberg, 1996; Iraqui *et al.*, 1999).

B. Detected radical amino acid changes in *S. uvarum* (Su) and *S. kudriavzevii* (Sk) compared to *S. cerevisiae* (Sc). *T. delbrueckii* (Td) sequence was used as an outgroup for the functional divergence analysis. Subscript numbers indicate the original amino acid position for each species. The alignment positions are relative to Su-Sc-Td and Sk-Sc-Td alignments respectively. Grantham's scores (Grantham, 1974) of the identified significant radical amino acid changes are shown.

phenylalanine as nitrogen source. In contrast, the strain ST44 showed a 63.9% and 91.3% reduction of PA and PEA production, respectively, compared to ST44-Sc. These data confirm the importance of the *ARO80* gene in PA and PEA production and demonstrate that *S. uvarum* and *S. kudriavzevii* *ARO80* alleles induce both PE and PEA increased production from the precursor phenylalanine.

Effect of the *ARO80* alleles in the *ARO9* and *ARO10* expression profiles

The results showed above might indicate differences in the regulation of the Aro80p target genes *ARO9* and *ARO10* by the non-*cerevisiae* *ARO80* alleles. Therefore, we tested the effect of the *ARO80* alleles on their expression pattern profiles in the presence of phenylalanine by taking samples at different times after cells were

inoculated into YNB 12.5 g l⁻¹ phenylalanine medium (Fig. 4, Table S3). Indeed, we observed that the expression of both *ARO9* and *ARO10* genes in the strain ST44-Su and ST44-Sk are two-fold higher than in the strain ST44-Sc after 10 h. However, no differences were observed between the *ARO80* recombinant strains after 24 h, except for a higher expression of *ARO9* in the strain ST44-Sk compared to ST44-Sc at 30 h. In contrast, and as expected, the mutant strain ST44 expressed both *ARO9* and *ARO10* genes but unable to induce their expression in the presence of phenylalanine during the whole experiment.

Discussion

Previous studies have demonstrated that *S. uvarum* and *S. kudriavzevii* produce higher amounts of PE and PEA than *S. cerevisiae* from the aromatic amino acid

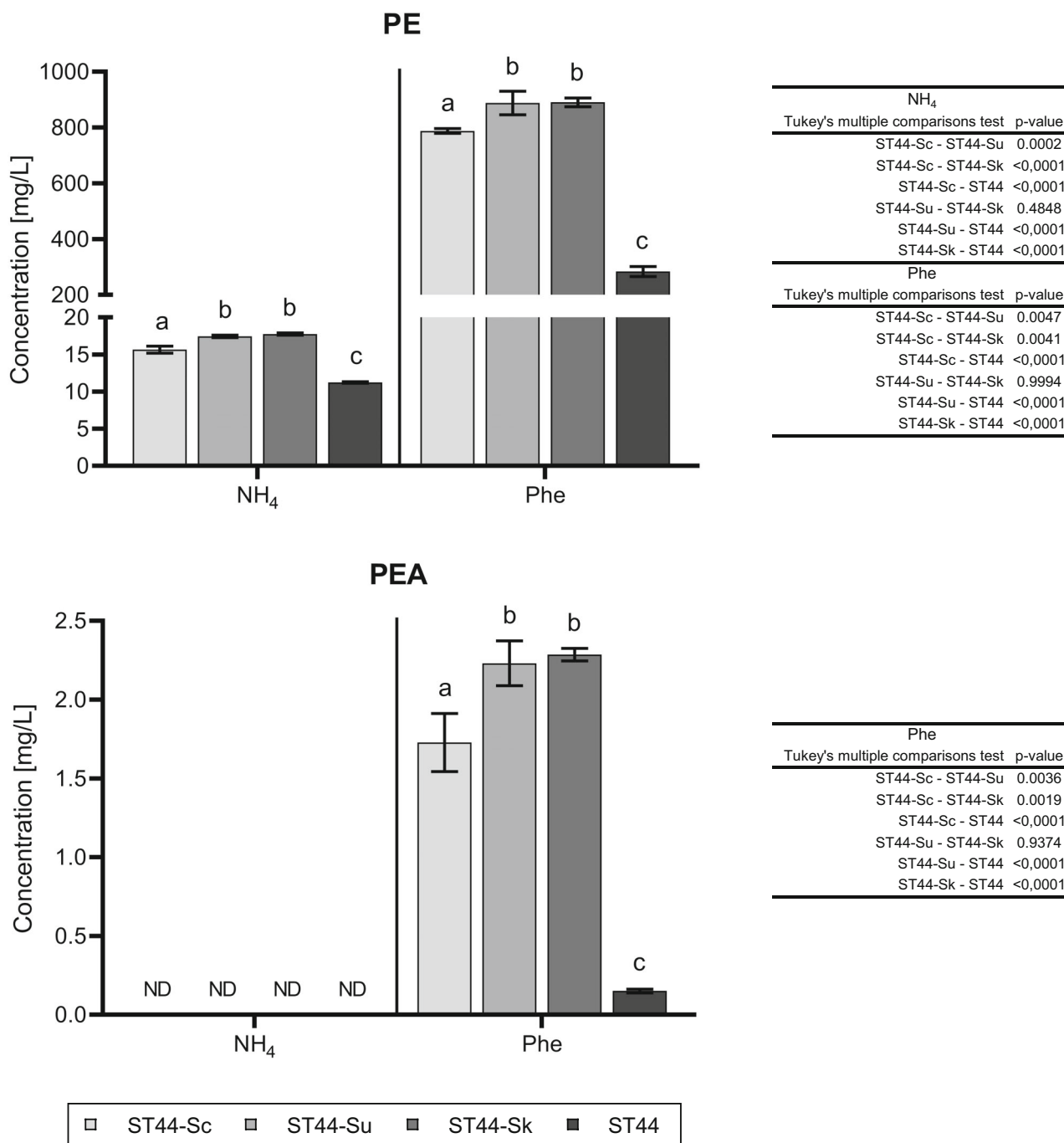


Fig. 3. Production of phenyl ethanol (PE) and phenylethyl acetate (PEA) by the recombinant *ARO80* strains in minimal medium. Either ammonium sulphate (NH₄) or phenylalanine (Phe) was used as sole nitrogen sources. Error bars represent the standard deviation from three biological replicates. Statistical differences were determined through ANOVA analysis independently for each nitrogen source. p-values for Tukey's comparisons test are indicated. ND, Not detected.

precursor phenylalanine when it was used as the sole nitrogen source (Stribny *et al.*, 2015), suggesting differences in the activity of the pathways involved in the production of aromatic compounds. An in-silico analysis based on Grantham's scoring plus experimental validation have demonstrated that *S. kudriavzevii* Aro10p and

S. kudriavzevii/S. *uvarum* acetyltransferases Atf1p and Atf2p contains significant amino acid changes which produced differences in their activity, substrate affinity and impacted the wine's aroma profile when they were expressed in a wine *S. cerevisiae* strain (Stribny *et al.*, 2016a,2016b). The binuclear cluster protein Aro80p

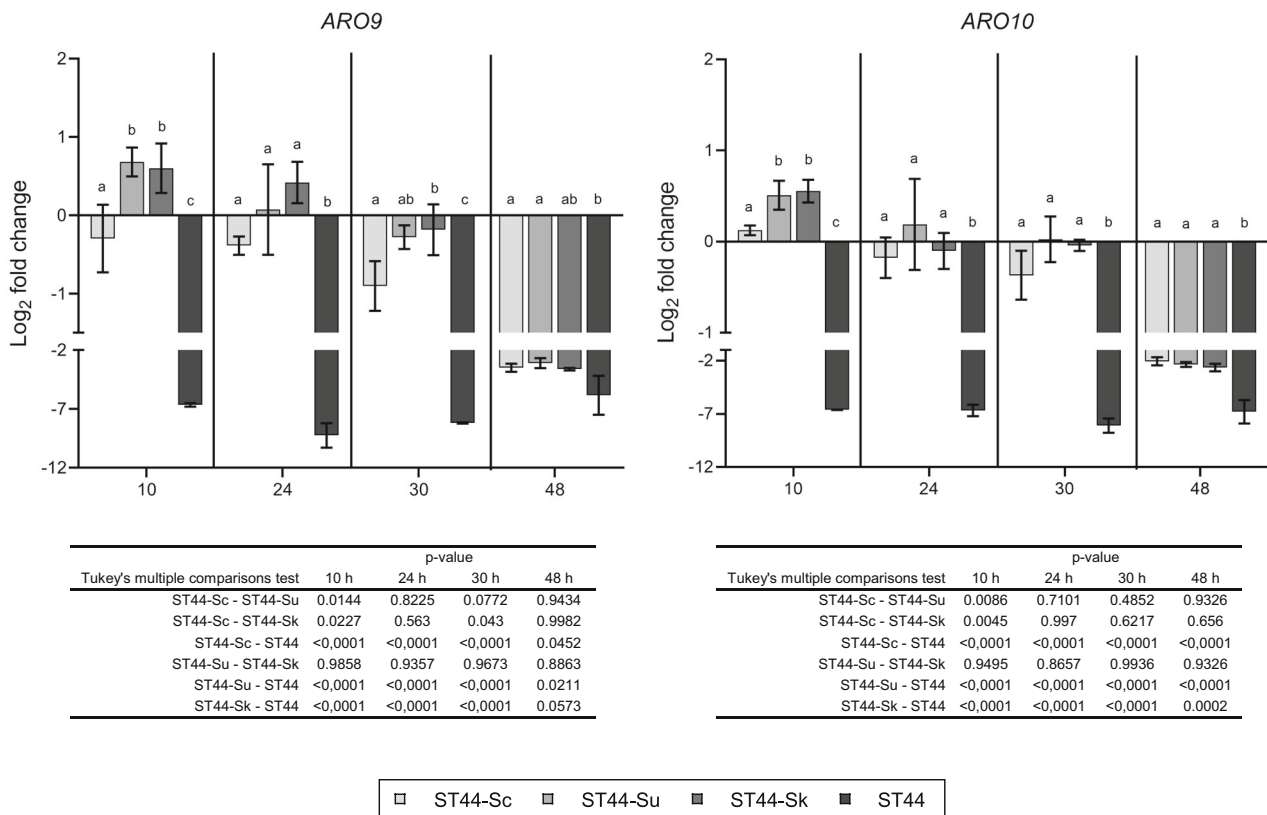


Fig. 4. Expression pattern of *ARO9* and *ARO10* genes of the *ARO80* recombinant strains cultured in minimal medium containing phenylalanine as the sole nitrogen source. Fold change was determined as the log-2 base logarithm of expression in one sample normalised against the average expression obtained at 10 h. Error bars represent the standard deviation from three biological replicates. Statistical differences were determined through ANOVA analysis independently for each time. p-values for Tukey's comparisons test are indicated.

showed the highest divergent scores in both *S. uvarum* and *S. kudriavzevii* (Stribny, 2016).

Since Aro80p regulates the expression of both Ehrlich pathway genes *ARO9* and *ARO10* (Iraqi *et al.*, 1999; Godard *et al.*, 2007), we studied the effect of the *S. uvarum* and *S. kudriavzevii* *ARO80* alleles (*ARO80*-Su and *ARO80*-Sk) on the PE and PEA production from the phenylalanine precursor. When these alleles were expressed in the wine *S. cerevisiae* strain T73, the PE and PEA production was increased compared to the *S. cerevisiae* wild-type allele (*ARO80*-Sc). Considering the regulatory function of Aro80p, we analysed the expression pattern of the Aro80p-regulated genes *ARO9* and *ARO10* at different times. It has been reported that overexpression of both genes increases the PE titer (Kim *et al.*, 2014). Indeed, the *ARO80*-Su and *ARO80*-Sk alleles induced higher expression levels of those genes in short times than the *ARO80*-Sc allele, which correlates with increased PE and PEA productions. Because only *ARO80* ORFs were swapped, their ability to induce higher expression levels might be explained by the identified amino acid changes. Aro80p belongs to the zinc

cluster proteins which are found exclusively in fungi and exhibit characteristic functional domains shared by the members of this family (Iraqi *et al.*, 1999; MacPherson *et al.*, 2006). However, since functional studies in *ARO80* have not been conducted yet, we came out with some suggestions based on published data. The substitution D₄₅A_{45/56} shared by both non-*cerevisiae* species is located at the loop that separates the two cysteine-rich substructures of the DNA-binding domain (DBD) metal-binding portion of the protein. Although Aro80p is constitutively bound to the UAS_{ARO} elements independently of the nitrogen source (Lee and Hahn, 2013) and the DBD is related only to the ability of the protein to bind to its cis element, it has been reported that similar changes in the regulatory protein Leu3p could improve not just the DNA-binding activity but also the transcriptional activity and therefore an increased expression *in vivo* of the regulated genes in the presence of the inducer (Bai and Kohlhaw, 1991). We observed many changes located in the middle region, between the DBD and activation domain (AD) in the proteins Aro80p-Su (Y₃₅₂C₃₆₇, N₅₀₂C₅₁₇ and G₆₉₀C₇₀₅) and Aro80p-Sk

(S₄₈₂I₄₈₆, R₄₈₈G₄₉₂, D₄₉₆A₅₀₀ and N₅₀₂Y₅₀₆). In most of the zinc cluster proteins, the region between these two domains contains a motif referred to as the middle homology region (MHR) and it is believed that it regulates the transcriptional activity of the protein (Schjerling and Holmberg, 1996; MacPherson *et al.*, 2006). Although Iraqui *et al.* (1999) reported a recognizable part of this motif in Aro80p between the positions 370 and 412, it seems to be absent and remains unclear which are the regulatory regions.

Some of the zinc cluster proteins that regulate the genes involved in the catabolism of specific amino acids act also as nutrient sensors (Sellick and Reece, 2005; MacPherson *et al.*, 2006). A well-reported case is the protein Put3p, which upregulates the expression of the proline catabolite genes *PUT1* and *PUT2* in the presence of the inducer proline as the sole nitrogen source. The proposed mechanism (Sellick and Reece, 2005) involves the interaction between Put3p and the proline to induce conformational changes which, in turn, unmask the AD that recruits the proteins to initiate the transcription. Indeed, it has been demonstrated that Put3p binds directly to proline through its pyrrolidine ring and then it induces the transcription of genes containing Put3p-binding sites (Sellick and Reece, 2003). A similar model has been hypothesised for the regulator Leu3p (Kohlhaw, 2003). Because the aromatic amino acids are the inducers of Aro80p, the same activation mechanism might be conserved, but a direct interaction has not been demonstrated yet (Lee and Hahn, 2013). The substitution G₅₃₂R in Put3p impairs the activation by proline without affecting the activity of other domains but an additional R₇₆₄T substitution not just recovers but increases the activity of Put3p, which becomes proline insensitive (Ann des Etages *et al.*, 1996). Other substitutions in the middle region have an impact on the AD masking which could produce either a permanent or loose unmasking that increases the transcription activity (Kohlhaw, 2003). Since the substitutions found in the Aro80p middle region are located at similar positions relative to the reported proteins, this suggests that such changes could affect the transcriptional activity by either changing a potential interaction between Aro80p and the phenylalanine or diminishing the AD masking. The substitution N₉₃₉I₉₅₄ is located at the C-terminal end of the AD in the Aro80p-Su and it probably exerts a minimal effect since the acidic/hydrophobic core (Schjerling and Holmberg, 1996) between positions 899 and 925 is conserved, and deletion experiments in Gal4p and Leu3p have demonstrated that the last twelve and nine residues, respectively, are dispensable for their transcriptional activities (Leuther *et al.*, 1993; Wang *et al.*, 1997). These results and suggested observations indicate that the different Aro80p proteins of this study could be used

as a model to identify the functional domains of the protein and promote future studies addressing how the different identified amino acid changes affect the Aro80p transcriptional activity.

Conclusions

In this study, we demonstrated that alleles *ARO80*-Su and *ARO80*-Sk increased both PEA and PE production compared to the strain carrying *ARO80*-Sc by enhancing the expression of the *ARO9* and *ARO10* genes in the presence of the inducer phenylalanine. We also identified candidate amino changes between Aro80p proteins that might explain differences in the expression of their target genes *ARO9* and *ARO10*. Finally, we propose that changes in the *ARO80* gene can be interesting to characterize the Aro80p regulatory domains, and with that, the developing of novel strains showing higher expression in *ARO9* and *ARO10* genes and, hence, increasing the PE and PEA production in wine.

Acknowledgements

This project has received funding from the European Union's Horizon 2020 research and innovation programme under the Marie Skłodowska-Curie grant agreement number 764364, Aromagenesis, and from the Spanish government and EU ERDF-FEDER projects RTI2018-093744-B-C31 and RTI2018-093744-B-C32 to AQ and EB respectively.

Conflict of interest

None declared.

References

- Ann des Etages, S. G. Fahey, D. A., Reecet, R. J., and Brandriss, M. C. (1996) Functional analysis of the *PUT3* transcriptional activator of the proline utilization pathway in *Saccharomyces cerevisiae*. *Genetics* **142**: 1069–1082.
- Bai, Y., and Kohlhaw, G.B. (1991) Manipulation of the 'Zinc cluster' region of transcriptional activator *LEU3* be site-directed mutagenesis. *Nucleic Acids Res* **19**: 5991–5997.
- Baudin, A., Ozier-kalogeropoulos, O., Denouel, A., Lacroute, F., and Cullin, C. (1993) A simple and efficient method for direct gene deletion in *Saccharomyces cerevisiae*. *Nucleic Acids Res* **21**: 3329–3330.
- Cordente, A.G., Curtin, C.D., Varela, C., and Pretorius, I.S. (2012) Flavour-active wine yeasts. *Appl Microbiol Biotechnol* **96**: 601–618.
- Doench, J.G., Hartenian, E., Graham, D.B., Tothova, Z., Hegde, M., Smith, I., *et al.* (2014) Rational design of highly active sgRNAs for CRISPR-Cas9-mediated gene inactivation. *Nat Biotechnol* **32**: 1262–1267.
- Gamero, A., Tronchoni, J., Querol, A., and Belloch, C. (2013) Production of aroma compounds by cryotolerant

- Saccharomyces* species and hybrids at low and moderate fermentation temperatures. *J Appl Microbiol* **114**: 1405–1414.
- Generoso, W.C., Gottardi, M., Oreb, M., and Boles, E. (2016) Simplified CRISPR-Cas genome editing for *Saccharomyces cerevisiae*. *J Microbiol Methods* **127**: 203–205.
- Gientka, I., and Duszkiwicz-Reinhard, W. (2009) Shikimate pathway in yeast cells: Enzymes, functioning, regulation - A review. *Polish J Food Nutr Sci* **59**: 113–118.
- Gietz, R.D., and Schiestl, R.H. (2007) Frozen competent yeast cells that can be transformed with high efficiency using the LiAc/SS carrier DNA/PEG method. *Nat Protoc* **2**: 1–4.
- Godard, P., Urrestarazu, A., Vissers, S., Kontos, K., Bontempo, G., van Helden, J., and Andre, B. (2007) Effect of 21 different nitrogen sources on global gene expression in the yeast *Saccharomyces cerevisiae*. *Mol Cell Biol* **27**: 3065–3086.
- Goffeau, A., Barrell, B.G., Bussey, H., Davis, R.W., Dujon, B., Feldmann, H., *et al.* (1996) Life with 6000 genes. *Science* **274**: 546–567.
- González, S.S., Gallo, L., Climent, M.D., Barrio, E., and Querol, A. (2007) Enological characterization of natural hybrids from *Saccharomyces cerevisiae* and *S. kudriavzevii*. *Int J Food Microbiol* **116**: 11–18.
- Gordon, J.L., Armisen, D., Proux-Wéra, E., ÓhÉigeartaigh, S.S., Byrne, K.P., and Wolfe, K.H. (2011) Evolutionary erosion of yeast sex chromosomes by mating-type switching accidents. *Proc Natl Acad Sci USA* **108**: 20024–20029.
- Grantham, R. (1974) Amino acid difference formula to help explain protein evolution. *Science* **185**: 862–864.
- Güldener, U., Heck, S., Fiedler, T., Beinhauer, J., and Hegemann, J.H. (1996) A new efficient gene disruption cassette for repeated use in budding yeast. *Nucleic Acids Res* **24**: 2519–2524.
- Hazelwood, L.A., Daran, J.-M., van Maris, A.J.A., Pronk, J.T., and Dickinson, J.R. (2008) The ehrlich pathway for fusel alcohol production: a century of research on *Saccharomyces cerevisiae* metabolism. *Appl Environ Microbiol* **74**: 2259–2266.
- Iraqi, I., Vissers, S., André, B., and Urrestarazu, A. (1999) Transcriptional induction by aromatic amino acids in *Saccharomyces cerevisiae*. *Mol Cell Biol* **19**: 3360–3371.
- Kim, B., Cho, B.R., and Hahn, J.S. (2014) Metabolic engineering of *Saccharomyces cerevisiae* for the production of 2-phenylethanol via Ehrlich pathway. *Biotechnol Bioeng* **111**: 115–124.
- Kohlhaw, G.B. (2003) Leucine biosynthesis in fungi: entering metabolism through the back door. *Microbiol Mol Biol Rev* **67**: 1–15.
- Lee, K., and Hahn, J.S. (2013) Interplay of Aro80 and GATA activators in regulation of genes for catabolism of aromatic amino acids in *Saccharomyces cerevisiae*. *Mol Microbiol* **88**: 1120–1134.
- Leuther, K.K., Salmeron, J.M., and Johnston, S.A. (1993) Genetic evidence that an activation domain of *GAL4* does not require acidity and may form a β sheet. *Cell* **72**: 575–585.
- Liti, G., Carter, D.M., Moses, A.M., Warringer, J., Parts, L., James, S.A., *et al.* (2009) Population genomics of domestic and wild yeasts. *Nature* **458**: 337–341.
- Macías, L.G., Flores, M.G., Adam, A.C., Rodríguez, M.E., Querol, A., Barrio, E., *et al.* (2021) Convergent adaptation of *Saccharomyces uvarum* to sulfite, an antimicrobial preservative widely used in human-driven fermentations. *PLoS Genet* **17**: e1009872.
- Macías, L.G., Morard, M., Toft, C., and Barrio, E. (2019) Comparative genomics between *Saccharomyces kudriavzevii* and *S. cerevisiae* applied to identify mechanisms involved in adaptation. *Frontiers in Genetics* **10**: 1–11.
- MacPherson, S., Laroche, M., and Turcotte, B. (2006) A fungal family of transcriptional regulators: the zinc cluster proteins. *Microbiol Mol Biol Rev* **70**: 583–604.
- Morard, M., Macías, L.G., Adam, A.C., Lairón-Peris, M., Pérez-Torrado, R., Toft, C., and Barrio, E. (2019) Aneuploidy and ethanol tolerance in *Saccharomyces cerevisiae*. *Frontiers in Genetics* **10**: 1–12.
- Pérez-Torrado, R., González, S.S., Combina, M., Barrio, E., and Querol, A. (2015) Molecular and enological characterization of a natural *Saccharomyces uvarum* and *Saccharomyces cerevisiae* hybrid. *Int J Food Microbiol* **204**: 101–110.
- Pérez-Torrado, R., Oliveira, B.M., Zemancíková, J., Sychrová, H., and Querol, A. (2016) Alternative glycerol balance strategies among *Saccharomyces* species in response to winemaking stress. *Front Microbiol* **7**: 1–13.
- Pretorius, I.S. (2000) Tailoring wine yeast for the new millennium: novel approaches to the ancient art of winemaking. *Yeast* **16**: 675–729.
- Qian, X., Yan, W., Zhang, W., Dong, W., Ma, J., Ochsenreither, K., *et al.* (2019) Current status and perspectives of 2-phenylethanol production through biological processes. *Crit Rev Biotechnol* **39**: 235–248.
- Querol, A., Huerta, T., Barrio, E., and Ramon, D. (1992) Dry yeast strain for use in fermentation of alicante wines: selection and DNA patterns. *J Food Sci* **57**: 183–185.
- Querol, A., Pérez-Torrado, R., Alonso-del-Real, J., Minebois, R., Stribny, J., Oliveira, B.M., and Barrio, E. (2018) New trends in the uses of yeasts in oenology. In *Advances in Food and Nutrition Research*. Amsterdam, Netherlands: Elsevier Inc., pp. 177–210.
- Rollero, S., Bloem, A., Ortiz-Julien, A., Bauer, F.F., Camarasa, C., and Divol, B. (2019) A comparison of the nitrogen metabolic networks of *Kluyveromyces marxianus* and *Saccharomyces cerevisiae*. *Environ Microbiol* **21**: 4076–4091.
- Scannell, D.R., Zill, O.A., Rokas, A., Payen, C., Dunham, M.J., Eisen, M.B., *et al.* (2011) The awesome power of yeast evolutionary genetics: new genome sequences and strain resources for the *Saccharomyces sensu stricto* genus. *G3: Genes, Genomes, Genetics* **1**: 11–25.
- Schjerling, P., and Holmberg, S. (1996) Comparative amino acid sequence analysis of the C6 zinc cluster family of transcriptional regulators. *Nucleic Acids Res* **24**: 4599–4607.
- Sellick, C.A., and Reece, R.J. (2003) Modulation of transcription factor function by an amino acid: activation of Put3p by proline. *EMBO J* **22**: 5147–5153.
- Sellick, C.A., and Reece, R.J. (2005) Eukaryotic transcription factors as direct nutrient sensors. *Trends Biochem Sci* **30**: 405–412.
- Stovicek, V., Holkenbrink, C., and Borodina, I. (2017) CRISPR/Cas system for yeast genome engineering: advances and applications. *FEMS Yeast Res* **17**: 1–16.

- Stribny, J. (2016) Genetic and molecular basis of the aroma production in *S. kudriavzevii*, *S. uvarum* and *S. cerevisiae*.
- Stribny, J., Gamero, A., Pérez-Torrado, R., and Querol, A. (2015) *Saccharomyces kudriavzevii* and *Saccharomyces uvarum* differ from *Saccharomyces cerevisiae* during the production of aroma-active higher alcohols and acetate esters using their amino acidic precursors. *Int J Food Microbiol* **205**: 41–46.
- Stribny, J., Querol, A., and Pérez-Torrado, R. (2016a) Differences in enzymatic properties of the *Saccharomyces kudriavzevii* and *Saccharomyces uvarum* alcohol acetyltransferases and their impact on aroma-active compounds production. *Front Microbiol* **7**: 1–13.
- Stribny, J., Romagnoli, G., Pérez-Torrado, R., Daran, J.M., and Querol, A. (2016b) Characterisation of the broad substrate specificity 2-keto acid decarboxylase Aro10p of *Saccharomyces kudriavzevii* and its implication in aroma development. *Microb Cell Fact* **15**: 1–12.
- Toft, C., Williams, T.A., and Fares, M.A. (2009) Genome-wide functional divergence after the symbiosis of proteobacteria with insects unraveled through a novel computational approach. *PLoS Comput Biol* **5**: 1–10.
- Ugliano, M., and Henschke, P.A. (2009) Yeasts and wine flavour. In *Wine Chemistry and Biochemistry*. Moreno-Arribas, M.V., and Polo, M.C. (eds). New York: Springer New York, pp. 313–392.
- Wang, D., Hu, Y., Zheng, F., Zhou, K., and Kohlhaw, G.B. (1997) Evidence that intramolecular interactions are involved in masking the activation domain of transcriptional activator Leu3p. *J Biol Chem* **272**: 19383–19392.

Supporting information

Additional supporting information may be found online in the Supporting Information section at the end of the article.

Fig. S1. Amplified *KanMX* cassette from plasmid pUG6 used to disrupt the *ARO80* gene in AQ2775 background. The PCR was carried out using the primers *aro80Δ*-Fw and *aro80Δ*-Rv. Ld: GeneRuler™ 1kb DNA ladder (Thermo Fisher Scientific, Waltham, MA, USA)

Fig. S2. Confirmation PCR of *ARO80* gene disruption. (Left): PCR performed using the diagnosis primers ARO80-Sc-test-Fw and K2. (Right): PCR carried out using the diagnosis primers ARO80-Sc-test-Fw and ARO80-Sc-test-Rv. C1-5: *aro80Δ* colonies, WT: Parental strain AQ2775, B: Negative control (water), Ld: GeneRuler™ 1kb DNA ladder (Thermo Fisher Scientific, Waltham, MA, USA).

Fig. S3. pRCC-N PCR product containing gRNA for *KanMX*. PCR was carried out using the protospacer incorporation primers gRNA-*KanMX*-Fw and gRNA-*KanMX*-Rv. Plasmid pRCC-N was used as a template. Ld: GeneRuler™ 1kb DNA ladder (Thermo Fisher Scientific, Waltham, MA, USA).

Fig. S4. *ARO80* alleles PCR products containing homologous sequences to *S. cerevisiae ARO80* locus. The PCR was carried out using the pair primers ARO80-Sc-Fw/ARO80-Sc-Fw, ARO80-Sk-Fw/ARO80-Sk-Fw and ARO80-Su-Fw/ARO80-Su-Fw to amplify the *ARO80* alleles from total DNA of the strains AQ2775, AQ4013, and AQ2901 respectively. Ld: GeneRuler™ 1kb DNA ladder (Thermo Fisher Scientific, Waltham, MA, USA).

Fig. S5. Confirmation PCR of *ARO80* allele swapping. The PCR confirmed the presence of *ARO80* alleles at the *S. cerevisiae ARO80* locus. The reverse primers are specific for each allele and a PCR for the *KanMX* cassette at the *ARO80* locus was done as control. C1-3: *ARO80*(Sc), C4-5: *ARO80*(Su), C6-9: *ARO80*(Sk), C10: *aro80*[ORF]::*KanMX*, C11: AQ2775, Ld: Invitrogen™ 100 bp DNA ladder (Thermo Fisher Scientific, Waltham, MA, USA).

Fig. S6. Integrated *ARO80* alleles amplification for Sanger sequencing. The PCR was carried out using the pair primers ARO80-Sc-test-Fw/ARO80-Sc-Rv2. The strains C2 (ST44-Sc), C4 (ST44-Su) and C6 (ST44-Sk) were confirmed as positive transformants and used for further experiments. C1-3: *ARO80*(Sc), C4-5: *ARO80*(Su), C6-9: *ARO80*(Sk), C10: *aro80*[ORF]::*KanMX*, C11: AQ2775, Ld: GeneRuler™ 1kb DNA ladder (Thermo Fisher Scientific, Waltham, MA, USA).

Table S1. Aro80p functional analysis results.

Table S2. Phenylethanol and phenylethyl acetate quantification data.

Table S3. *ARO9* and *ARO10* relative quantification data.